# Balanced between oxygen 2*p* holes and oxygen vacancies for optimal water oxidation

Gao Chen,*[1+] Yiran Ying,[2+] Sixuan She,[2] Yanping Zhu,[2] Zhiwei Hu,*[3] Jiayi Tang,[4] Xubin Ye,[5] Youwen Long, [5] Chang-Yang Kuo[6,7], Chien-Te Chen,[6] Dongsheng Geng,[1] Haitao Huang,*[2] Zongping Shao*[4]

[1]Jiangsu Key Laboratory of New Energy Devices and Interface Science, School of Chemistry and Materials Science, Nanjing University of Information Science and Technology, Nanjing, 210044, China

[2]Department of Applied Physics and Research Institute for Smart Energy, The Hong Kong Polytechnic University, Hong Kong, China

[3]Max-Planck-Institute for Chemical Physics of Solids, Nöthnitzer Street 40, Dresden 01187, Germany

[4]WA School of Mines: Minerals, Energy and Chemical Engineering, Curtin University, Perth WA 6102, Australia

[5]Beijing National Laboratory for Condensed Matter Physics, Institute of Physics, Chinese Academy of Sciences, Beijing 100190, China

[6]National Synchrotron Radiation Research Center, 101 Hsin-Ann Road, Hsinchu 30076, Taiwan, R.O.C

[7]Department of Electrophysics, National Yang Ming Chiao Tung University, Hsinchu 300, Taiwan, R.O.C

**Synthesis of $Sr_{(1-x)}Y_xCoO_{3-\delta}$ perovskite powders under atomosphere pressure**

$Sr_{(1-x)}Y_xCoO_{3-\delta}$ ($x$=0, 0.1, 0.2, and 0.3) powders were synthesized using a conventional solid-state reaction method. Briefly, stoichiometric amounts of $SrCO_3$, $Co_3O_4$, and $Y_2O_3$ (Sigma-Aldrich Corporation) were mixed in mortar for 1 h. The mixed precursors were finally calcined in ambient air in box furnaces at 950 °C for 12 h for SC and 1100 °C for 12 h for others.

**Synthesis of $Sr_{(1-x)}Y_xCoO_{3-\delta}$ perovskite powders under high pressure**

$Sr_{(1-x)}Y_xCoO_{3-\delta}$ (x=0, 0.5, and 1, denoted as SC-HP, S0.5Y0.5C-HP, and YC-HP, respectively) samples were synthesized via a solid-state reaction under high-pressure and high-temperature conditions. The synthesis route is illustrated by taking SC-*HP* as an example. High purity (> 99.9%) fine powders of SrO, $Co_3O_4$, and $KClO_4$ were used as starting materials, and thoroughly mixed with a stoichiometric molar ratio of 3:1:1 in an agate mortar within an argon-filled glove box. The SrO precursor was obtained by firing $SrCO_3$ at 1273 K for 12 h in air. The excessive $KClO_4$ could provide an adequate oxygen environment. Finely mixed reactants were sealed into a Pt capsule of diameter 3 mm and length 4 mm, which was put into a BN sleeve and then inserted into a cylindrical graphite heater, with both ends in contact with Mo disks. A cube of pyrophyllite acted as the pressure medium. The capsulated samples were treated at 7 GPa and 1473 K for 30 minutes on a cubic-anvil-type high-pressure apparatus. Once the heating was finished, the sample was quenched to room temperature before the slow release of pressure over several hours. The as-made polycrystalline pellet was ground, and rinsed with deionized water to remove the residual KCl.

**Characterizations**

The XRD patterns were captured on a Rigaku Smartlab with filtered Cu-Kα radiation (λ = 1.5418 Å). The diffraction patterns were collected by scanning in a 2θ range of 20–80° with a step of 0.02°. The specific surface areas of the catalysts were obtained with a Brunauer-Emmett-Teller (BET) analysis system with a $N_2$ adsorptive medium. $N_2$ adsorption-desorption isotherms of the catalysts were measured at -196 °C using ASAP Tristar II 3020. The Co-$L_{2,3}$ and O-$K$ XAS spectra were taken in the total electron yield mode at the BL 11A in National Synchrotron

Radiation Research Center (NSRRC) in Taiwan, probing the top ≈5 nm of the sample surface.

**Electrode preparation and electrochemical characterization**

Electrochemical measurements were performed at room temperature using a rotating disk working electrode made of glassy carbon (PINE, 5 mm diameter, 0.196 $cm^2$) connected to a Bio-Logic (SP-150) electrochemical station. The glassy carbon (GC) electrode was pre-polished with 50 nm α-$Al_2O_3$ slurries on a polishing cloth and sonicated in ethanol for 5 min. The electrodes were finally rinsed with deionized water and dried before each test. A Pt foil and Hg/HgO were used as the counter and reference electrodes, respectively. The potentials reported in our work are referenced to the reversible hydrogen electrode (RHE). The preparation method of the working electrodes containing the investigated catalysts is as follows. To remove any electrode conductivity limitation present in the thin film electrodes, all the catalysts were mixed with as-received conductive carbon (Super P Li). Briefly, a mixture of oxide (18 mg) and conductive carbon (3 mg) were dispersed in a 3 mL mixed DI-water/Nafion (5 wt%) solution with a volume ratio of 10/1. Then the mixture was sonicated for 30 min to generate a homogeneous ink. Next, a 10 μL aliquot of the as-prepared ink was dropped onto the surface of the RDE, yielding an approximate catalyst loading of 0.306 mg $cm^{-2}$) and left to dry for the OER tests. Cyclic voltammograms (CVs) were performed at the RDE at 1600 rpm in an $O_2$-saturated 0.1 M KOH solution (99.99% metal purity) at a scan rate of 10 mV $s^{-1}$ from 0 to 1.0 V versus Hg/HgO. All potential values were iR-corrected to compensate for the effect of the solution resistance, which was calculated by the following equation: $E_{iR\text{-}corrected} = E - iR$, where i is the current and R is the uncompensated ohmic electrolyte resistance measured via the high-frequency ac impedance in $O_2$-saturated 0.1 M KOH. The obtained CV curves were calibrated by averaging the curves derived from the positive and negative scans.

**Isotope-Labeled Method**

Firstly, A carbon paper with catalysts (2 mg $cm^{-2}$) was activated in $^{18}O$ labeled 1.0 M KOH for 10 min at 10 mA $cm^{-2}$. Then, the carbon paper was carefully washed with $H_2{}^{16}O$ deionized water to remove surface $H_2{}^{18}O$. Finally, the carbon paper was measured for three CV cycles in 1.0 m KOH with $H_2{}^{16}O$. The CV test was performed at a scan rate of 4 mV $s^{-1}$ between 0 V and 0.7 V versus Ag/AgCl. All the tests were carried out in an H-cell. The gaseous products from

the anode side were analyzed by mass spectrometry.

**Turnover frequency (TOF) calculations**

The TOF was calculated according to the equation:

$$TOF = \frac{j * A}{4nF}$$

where F is the Faraday constant (96485 C $mol^{-1}$); $j$ is the current density (mA $cm_{ox}^{-2}$) obtained at overpotential (η) = 350 mV vs. RHE; A is the catalyst's BET surface area and n is the number of active sites. As a usual practice,[1] the top 5 nm on the surface and the whole catalysts were considered for the surface and bulk calculations, respectively.

**Alkaline anion exchange membrane water electrolysis test**

The $S_{0.9}Y_{0.1}C$ and commercially available $IrO_2$ and Pt catalysts were mixed with water, conductive carbon, and a binder. The catalyst ink mixture was then sprayed onto a gas diffusion layer (GDL) substrate by using a spray gun. Electrodes typically contain 1 mg $cm^{-2}$ total catalyst loading. The cathode GDL is carbon paper, while the anode GDL is made of a titanium porous transport layer. The effective surface area of the GDL is 1 $cm^2$. The cells were assembled by placing appropriate gas diffusion electrodes on each side of the AEM. Sustainion X37 anion membrane was used throughout the work. The activity and stability of AEM water electrolysis were performed at 50 °C.

**Computational Details**

All the spin-polarized density functional theory (DFT) calculations were performed within the VASP code with the projector-augmented wave method.[2,3] The kinetic energy cutoff was set as 400 eV, and the energy and force convergence criteria were set as $10^{-5}$ eV and 0.02 eV/Å, respectively. Hubbard U framework[4] was used for correcting the self-interaction error in strongly correlated Co ions, while the U value was set as 3.32 eV.[5] 2×2×1 Monkhorst-Pack k-points meshes were used for Brillouin zone sampling. Vacuum layers with a thickness of more than 15 Å were used to avoid spurious interactions between adjacent image cells.

The Gibbs free energy change of each elementary step was calculated as $\Delta G = \Delta E + \Delta ZPE + \Delta H_{0\rightarrow T} - T\Delta S$, where ΔE, ΔZPE, $\Delta H_{0\rightarrow T}$, and TΔS are the differences in DFT-calculated energy,

zero-point energy, reaction enthalpy change from zero to finite temperature T, and entropic contribution (T=298 K), respectively. The pH correction was calculated as $\Delta G_{pH} = -k_B T \ln 10 * pH$. Nørskov's computational hydrogen electrode (CHE) model[6] was used in the calculations assuming $G(H^+ + e^-) = 0.5G(H_2, g) - eU$, where U is the applied potential.

ΔG for each elementary step in OER was calculated relative to the chemical potential of $H_2O$ and $H_2$ molecules. To be more specific, for the LOM_Co site (Figure 3a-b), ΔG values for each step were calculated as (here, the asterisk denotes the Co site, and $O_{vac}$ denotes the adjacent oxygen vacancy site):

$$\Delta G_1 = G(*OO\text{-}O_{vac}) - G(*OH) + 1/2\mu_{H2}$$

$$\Delta G_3 = G(*OH\text{-}H) - G(*OH\text{-}O_{vac}) - (\mu_{H2O} - 1/2\mu_{H2})$$

$$\Delta G_4 = G(*OH) - G(*OH\text{-}H) + 1/2\mu_{H2}$$

$$\Delta G_2 = 4.92\ (eV) - \Delta G_1 - \Delta G_3 - \Delta G_4$$

And for the LOM_O site (Figure 3c-d), ΔG values for each step were calculated as (here, the asterisk denotes the O site, and $O_{vac}$ denotes a vacancy at the O site):

$$\Delta G_1 = G(*OH) - G(*) - (\mu_{H2O} - 1/2\mu_{H2})$$

$$\Delta G_2 = G(*O) - G(*OH) + 1/2\mu_{H2}$$

$$\Delta G_4 = G(*H) - G(*O_{vac}) - (\mu_{H2O} - 1/2\mu_{H2})$$

$$\Delta G_5 = G(*) - G(*H) + 1/2\mu_{H2}$$

$$\Delta G_3 = 4.92\ (eV) - \Delta G_1 - \Delta G_2 - \Delta G_4 - \Delta G_5$$

We used the fixed total energy barrier of 4.92 eV for OER due to the inaccurate description of the molecular energy of $O_2$ by periodic DFT.

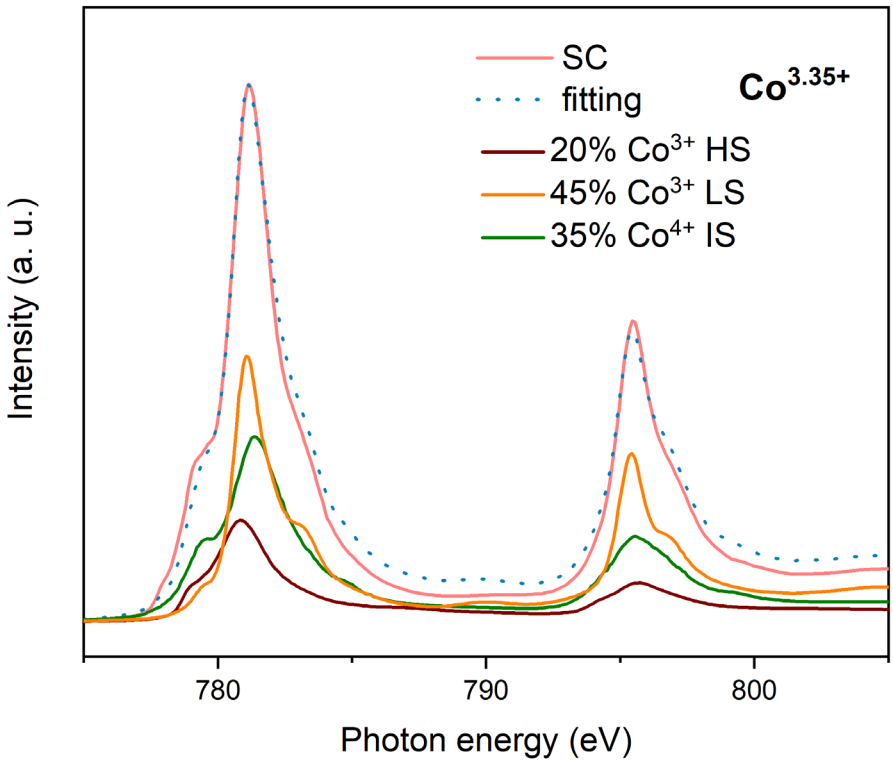


**Figure S1**. Fitting profile of Co-L edge in SC by superposition of the references: $EuCoO_3$ as LS $Co^{3+}$, $Sr_2CoO_3Cl$ as HS $Co^{3+}$ and $SrCoO_3$ as IS $Co^{4+}$.

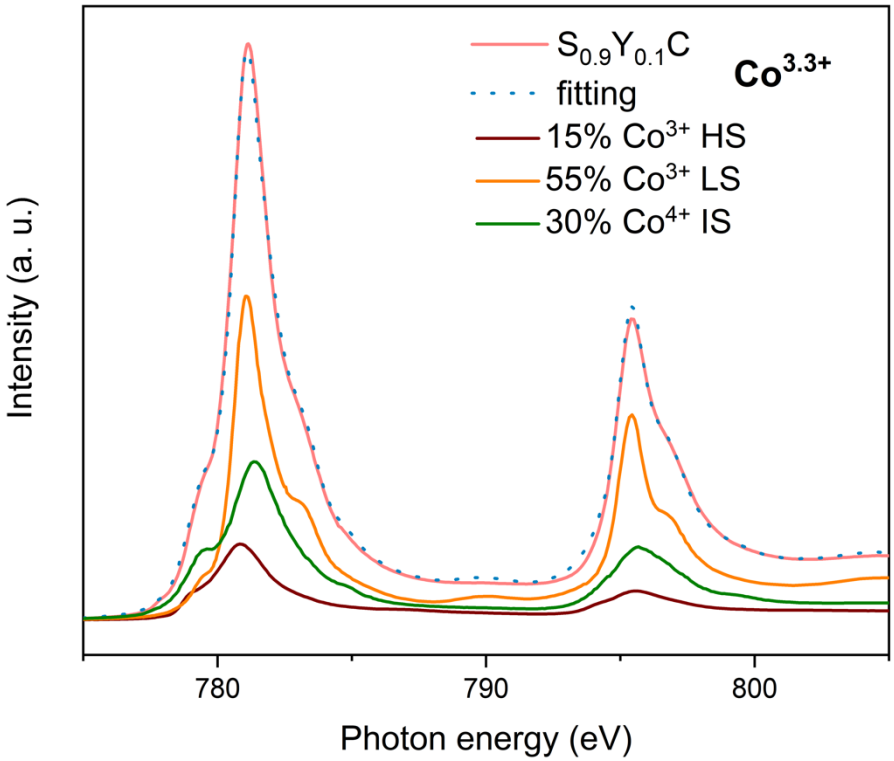


**Figure S2**. Fitting profile of Co-L edge in $S_{0.9}Y_{0.1}C$ by superposition of the references: $EuCoO_3$ as LS $Co^{3+}$, $Sr_2CoO_3Cl$ as HS $Co^{3+}$ and $SrCoO_3$ as IS $Co^{4+}$.

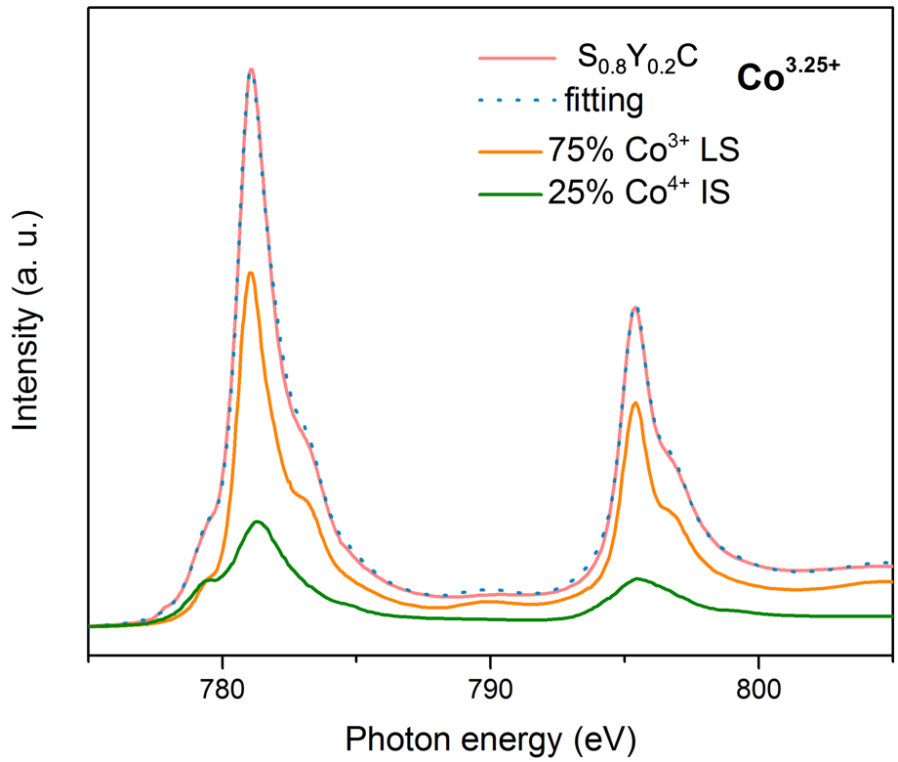


**Figure S3**. Fitting profile of Co-L edge in $S_{0.8}Y_{0.2}C$ by superposition of the references: $EuCoO_3$ as LS $Co^{3+}$ and $SrCoO_3$ as IS $Co^{4+}$.

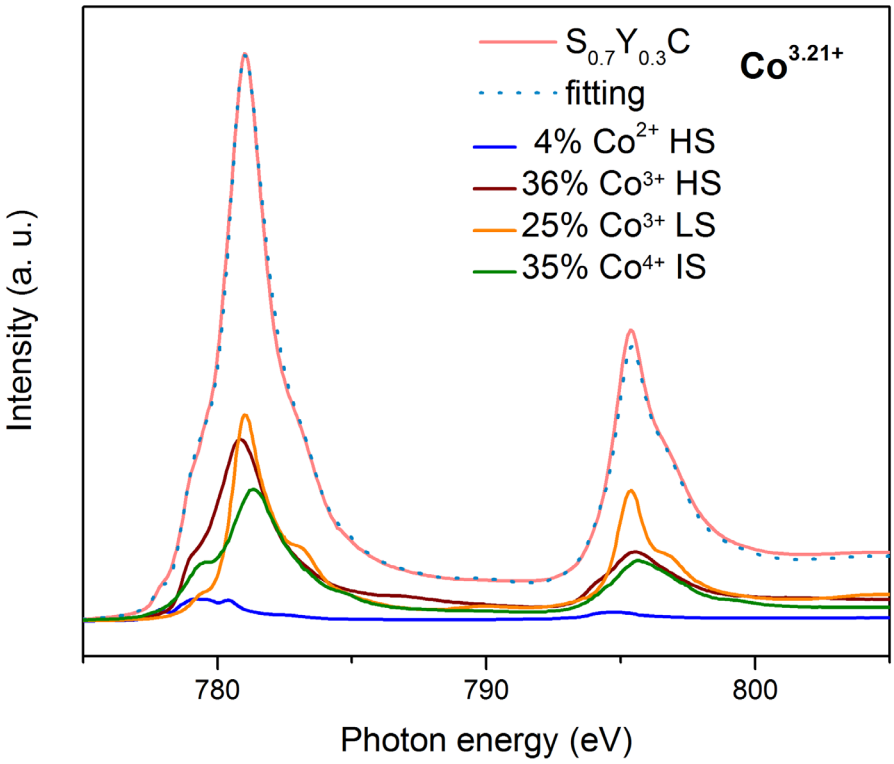


**Figure S4**. Fitting profile of Co-L edge in $S_{0.7}Y_{0.3}C$ by superposition of the references: CoO as HS $Co^{2+}$, $EuCoO_3$ as LS $Co^{3+}$, $Sr_2CoO_3Cl$ as HS $Co^{3+}$ and $SrCoO_3$ as IS $Co^{4+}$.

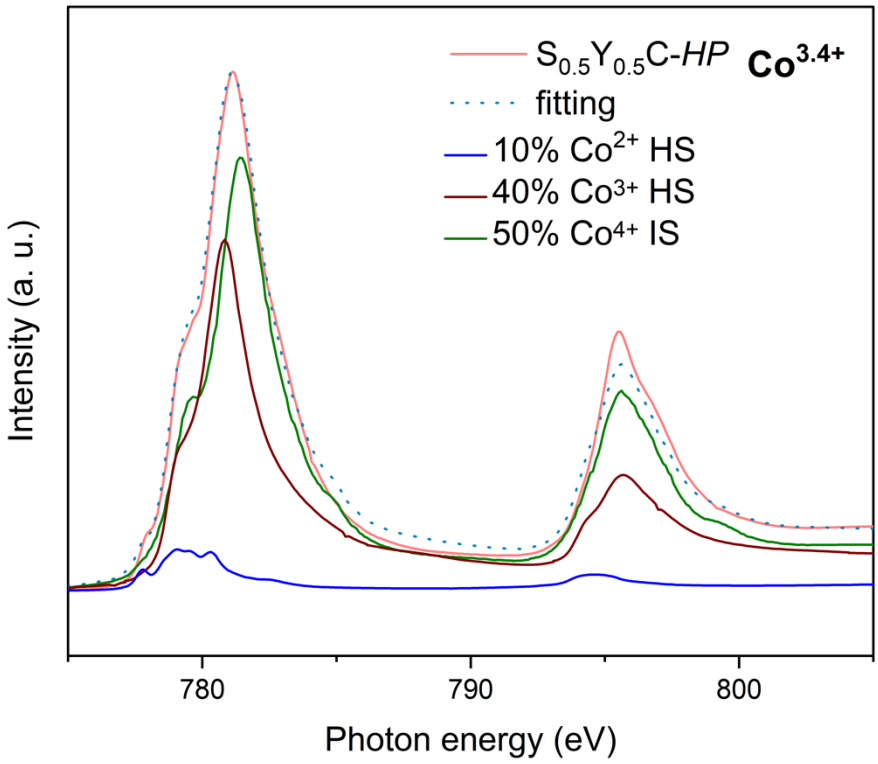


**Figure S5**. Fitting profile of Co-L edge in $S_{0.5}Y_{0.5}C$-*HP* by superposition of the references: $Sr_2CoO_3Cl$ as HS $Co^{3+}$ and $SrCoO_3$ as IS $Co^{4+}$.

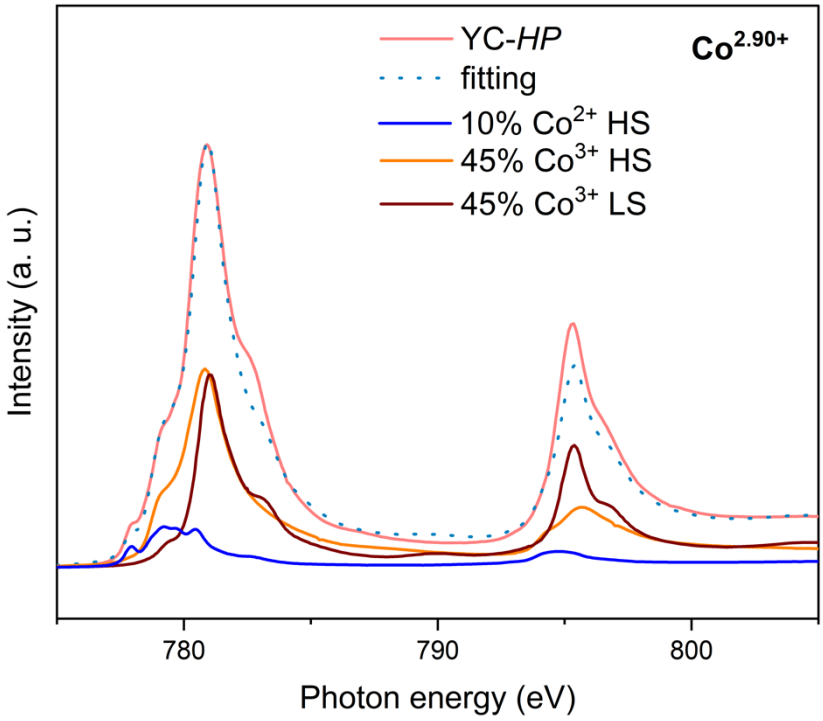


**Figure S6**. Fitting profile of Co-L edge in YC-*HP* by superposition of the references: CoO as HS $Co^{2+}$, $EuCoO_3$ as LS $Co^{3+}$ and $Sr_2CoO_3Cl$ as HS $Co^{3+}$.

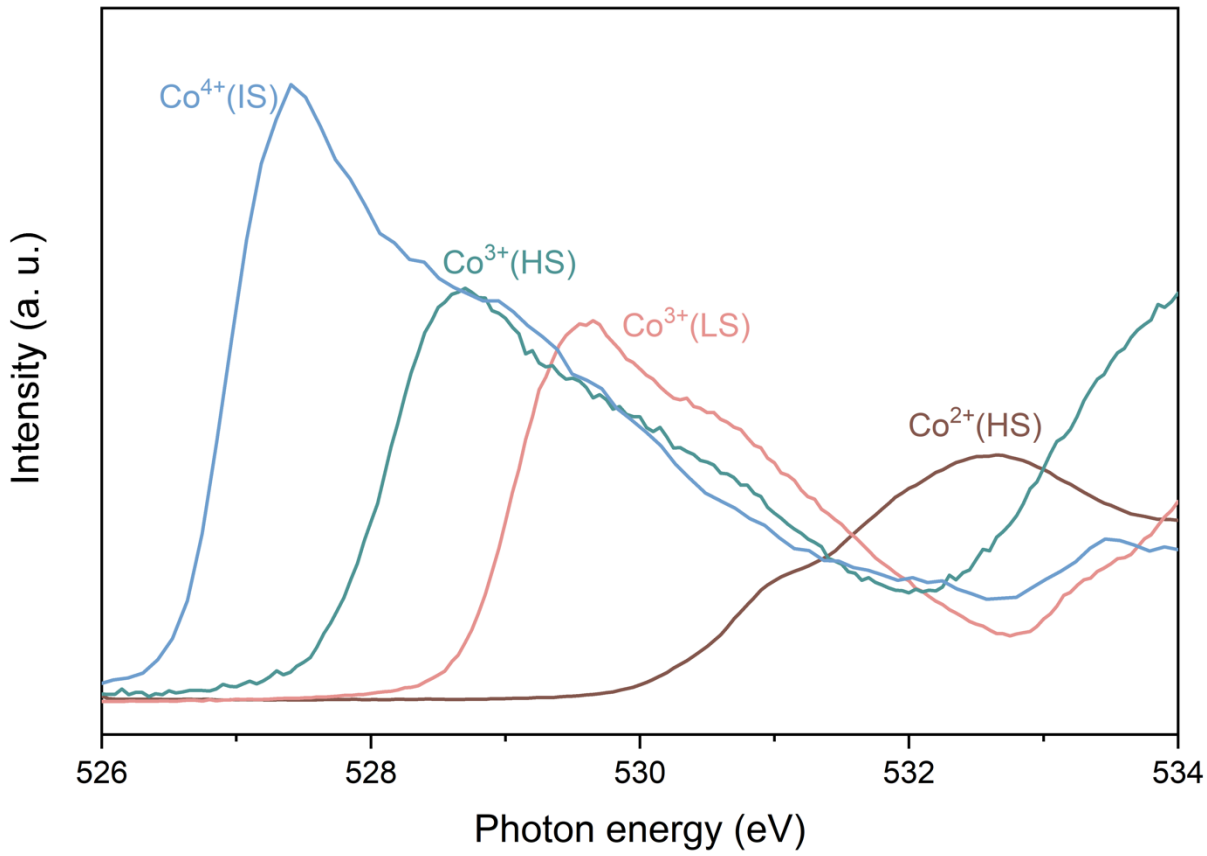


**Figrue S7.** The pre-edge peak of the O *K*-edge spectra of the four references including CoO (HS-$Co^{2+}$), $LaCoO_3$-20K (LS-$Co^{3+}$), $LaCoO_3$-650K (HS-$Co^{3+}$) and $SrCoO_3$ (IS-$Co^{4+}$).

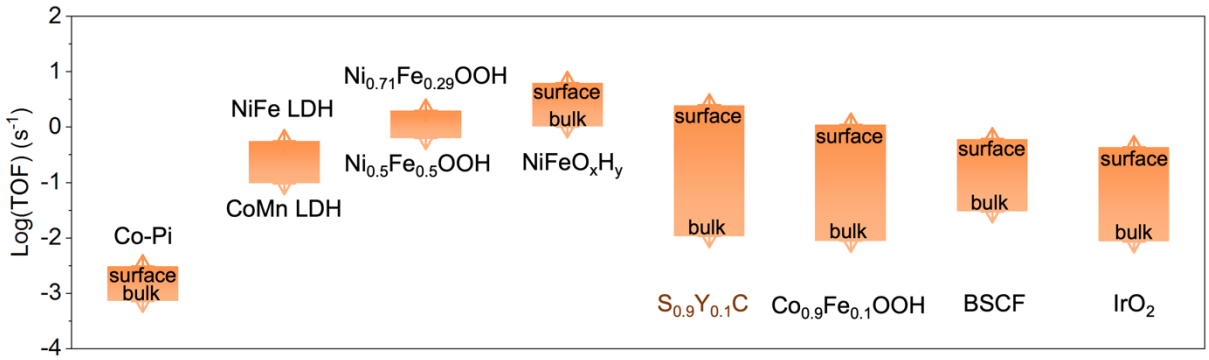


**Figure S8**. TOF comparison between $S_{0.9}Y_{0.1}C$, and some state-of-the-art catalysts, including Co-Pi, [7] NiFe LDH, [8] CoMn LDH, [9] $Ni_{0.71}Fe_{0.29}OOH$, [10] $Ni_{0.5}Fe_{0.5}OOH$, [10] 5.4 nm $NiFeO_xH_y$, [11] $Co_{0.9}Fe_{0.1}OOH$, [12] BSCF [13] and $IrO_2$ [14].

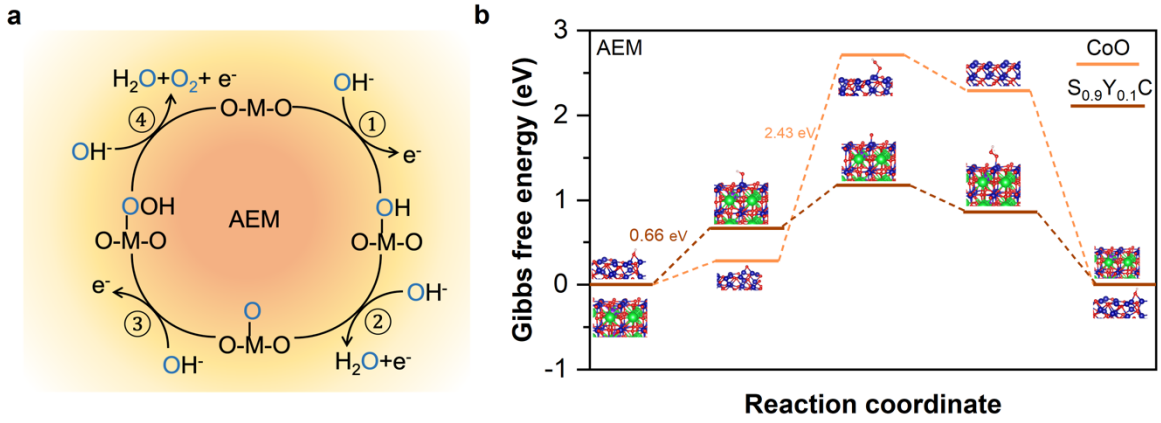


**Figure S9**. (**a**) Schematic illustration of AEM pathway of OER in alkaline conditions. (**b**) Gibbs free energy diagram of OER on CoO and $S_{0.9}Y_{0.1}C$ at applied potential U=1.23 V via AEM pathway. The optimized intermediate structures are shown as insets (color code: green for Sr, purple for Y, blue for Co, red for O, and pale pink for H).

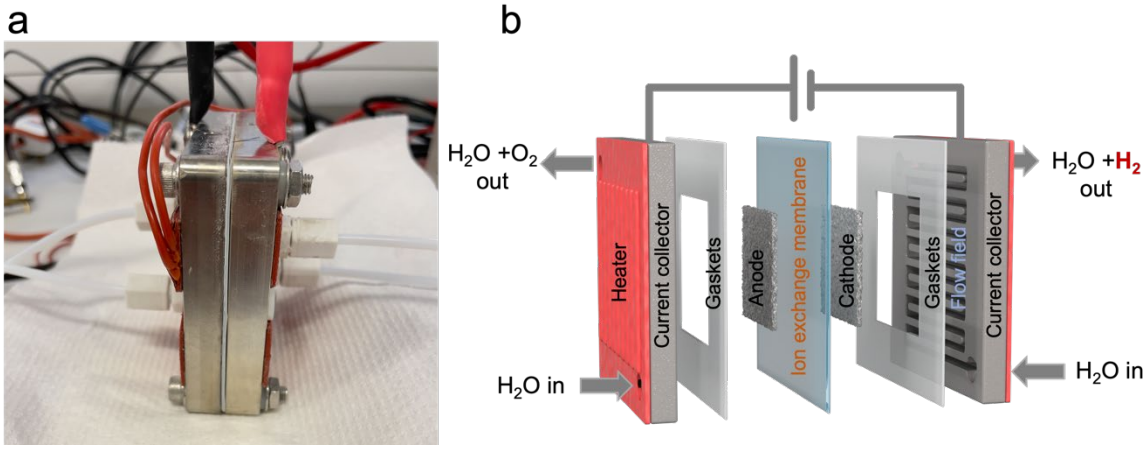


**Figure S10.** (a) Digital photograph and (b) schematic of the anion exchange membrane electrolyzer.

**Table S1**. Specific surface areas of the as-prepared samples measured by nitrogen adsorption testing using the BET method.

| Sample | BET surface area/($m^2$ $g^{-1}$) |
|---|---|
| SC-*HP* | 0.2394 |
| SC | 0.6294 |
| $S_{0.9}Y_{0.1}C$ | 0.1110 |
| $S_{0.8}Y_{0.2}C$ | 0.2295 |
| $S_{0.7}Y_{0.3}C$ | 0.1995 |
| $S_{0.5}C_{0.5}C$-*HP* | 0.2596 |
| YC-*HP* | 0.6757 |
| CoO | 1.0955 |

## Reference


[1] Chen, R.R.; Chen, G.; Ren, X.; Ge, J.; Ong, S.J.H.; Xi, S.; Wang, X.; Xu, Z.J., *Angew. Chem. Inter. Ed.* **2021**, 60, 25884-25890.

[2] Kresse, G.; Furthmüller, J., *Phys. Rev. B* **1996**, 54, 11169.

[3] Kresse, G.; Joubert, D., *Phys. Rev. B* **1999**, 59, 1758.

[4] Anisimov, V. V.; Zaanen, J.; Andersen, O. K., *Phys. Rev. B* **1991**, 44, 943-954.

[5] Jain, A.; Ong, S. P.; Hautier, G.; Chen, W.; Richards, W. D.; Dacek, S.; Cholia, S.; Gunter, D.; Skinner, D.; Ceder, G.; Persson, K. A., *APL Materials* **2013**, 1, 011002.

[6] Nørskov, J. K.; Rossmeisl, J.; Logadottir, A.; Lindqvist, L.; Kitchin, J. R.; Bligaard, T.; Jonsson, H., *J. Phys. Chem. B* **2004**, 108, 17886-17892.

[7] Surendranath, Y.; Kanan, M. W.; Nocera, D. G.; *J. Am. Chem. Soc.* **2010**, *132*, 16501-16509.

[8] Gong, M.; Li, Y.; Wang, H.; Liang, Y.; Wu, J. Z.; Zhou, J.; Wang, J.; Regier, T.; Wei, F.; Dai, H.; *J. Am. Chem. Soc.* **2013**, *135*, 8452-8455.

[9] Song, F.; Hu, X.; *J. Am. Chem. Soc.* **2014**, *136*, 16481-16484.

[10] Zaffran, J.; Stevens, M. B.; Trang, C. D.; Nagli, M.; Shehadeh, M.; Boettcher, S. W.; Toroker, M. C.; *Chem. Mater.* **2017**, *29*, 4761-4767.

[11] Roy, C.; Sebok, B.; Scott, S.; Fiordaliso, E.; Sørensen, J.; Bodin, A.; Trimarco, D.; Damsgaard, C.; Vesborg, P.; Hansen, O.; Stephens, I. E. L.; Kibsgaard, J.; Chorkendorff, I.; *Nat. Catal.* **2018**, *1*, 820-829.

[12] Wu, T.; Ren, X.; Sun, Y.; Sun, S. Xian, G.; Scherer, G. G.; Fisher, A. C.; Mandler, D.; Ager, J. W.; Grimaud, A.; Wang, J.; Shen, C.; Yang, H.; Gracia, J.; Gao, H.-J.; Xu Z. J.; *Nat. Commun.* **2021**, 12, 1-11.

[13] Hong, W. T.; Risch, M.; Stoerzinger, K. A.; Grimaud, A.; Suntivich, J.; Shao-Horn, Y.; *Energy Environ. Sci.* **2015**, *8*, 1404-1427.

[14] Trotochaud, L.; Ranney, J. K.; Williams, K. N.; Boettcher, S. W.; *J. Am. Chem. Soc.* **2012**, *134*, 17253-17261.